AIAA JOURNAL
Vol. 32, No. 8, August 1994

Effect of Orifice Flow and Heat Transfer on Gas Spring Hysteresis

Harold Mirels*
The Aerospace Corporation, El Segundo, California 90245

The combined effect of orifice flow and heat transfer on piston power dissipation within a gas spring has been evaluated within the framework of a small perturbation theory. The relationship between piston displacement and gas spring pressure perturbation has been deduced. Numerical results are presented for the effect of orifice flow and heat transfer on piston power, normalized with respect to piston displacement. The variation of normalized piston power $\bar{P}$ with orifice flow parameter K, at a fixed heat transfer, has a local maximum. When operating at the value of K corresponding to the local maximum in $\bar{P}$, the effect of heat transfer is to decrease $\bar{P}$. The variation of $\bar{P}$ with heat transfer, at fixed K, has been evaluated for a parallel-plate geometry and specific heat equal to $\gamma = 7/5$ and 5/3. In the absence of an orifice ($K = 0$), the optimum heat transfer provides, for $\gamma = 7/5$ and 5/3, a peak power equal to 22 and 30%, respectively, of peak power associated with optimum K and no heat transfer.

Nomenclature

A_1, A_2	= cross-sectional area at stations 1 and 2, Fig. 1
a	= function of y, Eq. (8)
b	= function of y, Eq. (8)
c_p	= specific heat at constant pressure
c_v	= specific heat at constant volume
E	= internal energy of gas in spring
G	= constant, Eq. (7)
K	= orifice flow parameter, Eq. (14)
L	= orifice length, Eq. (14)
L_1, L_2	= characteristic cavity lengths V_0/A_1, V_0/A_2
P	= average piston power
$\bar{P}$	= normalized average piston power, Eq. (23)
p	= pressure
p_1	= amplitude of pressure perturbation, Eq. (4)
Q	= net heat transfer from wall to gas
r	= semiwidth or radius, Fig. 2
S	= internal surface area in gas spring
s	= distance from centerline, Fig. 2
T	= gas temperature, K
t	= time
V	= volume of gas spring
v	= fluid velocity in s direction, Fig. 2
X_1	= complex amplitude of piston displacement, Eq. (16)
y	= normalized gas spring semiwidth parameter, r/λ
z	= $(1 + i)y$
α	= function defined in Eq. (19)
$\bar{\alpha}$	= thermal diffusivity, $k/(\rho c_p)$
β	= function defined in Eq. (19)
γ	= ratio of specific heats, c_p/c_v
$\Delta X_1, \Delta X_2$	= particle (piston) displacement at stations 1 and 2, Fig. 1
$\Delta( )$	= perturbation
λ	= characteristic thermal boundary-layer thickness $(2\bar{\alpha}/\omega)^{1/2}$
ρ	= density
μ	= viscosity
ν	= frequency, cycles/s
Φ	= phase of piston displacement relative to pressure perturbation, Eq. (20)
Φ_q	= phase of heat transfer rate (from gas to wall) relative to pressure perturbation, Eq. (6)
ω	= frequency, rad/s

Subscripts

m	= associated with maximum power dissipation, Eqs. (27–29)
0	= average conditions
1, 2	= conditions at stations 1 and 2, Fig. 1

Superscripts

$(\dot{})$	= $d( )/dt$
$( )^*$	= complex conjugate

Received Dec. 16, 1992; revision received Sept. 20, 1993; accepted for publication Oct. 10, 1993.

*Principal Scientist, Mechanics and Materials Technology Center. Fellow AIAA.

Introduction

GAS springs are devices wherein the compressibility of an enclosed gas retards piston motion by a force that is proportional to piston displacement. If gas-viscosity and heat-conduction effects are neglected, there are no gasdynamic losses associated with the piston motion. It is well known, however, that periodic piston motion results in a net heat transfer to the wall and, therefore, a finite expenditure of power (i.e., "hysteresis" effect). This phenomenon is well described in Ref. 1 for the entire range $0 < r/\lambda < \infty$. The effect of heat transfer on gas spring hysteresis was investigated experimentally in Ref. 2, and the results agree with the theoretical model of Ref. 1.

A major application of gas spring hysteresis theory is to the analysis of free-piston Stirling engines and cryocoolers.[3,4] The gas spring influences the phase difference between the free piston and a crankshaft-driven piston and, thereby, affects device performance. Increased hysteresis losses lead to increased refrigeration.[5]

A recent innovation in the design of Stirling cryocoolers is the replacement of the free piston and gas spring by a "pulse tube." Performance of pulse tube cryocoolers is enhanced by the presence of an orifice that permits periodic mass transport into and out of the tube.[6,7] This suggests that a study be undertaken of the combined effect of orifice flow and heat transfer on gas spring hysteresis. Such a study is conducted herein with emphasis on conditions that lead to maximum power dissipation. Small perturbations are assumed. The application to pulse tube cryocoolers is presented in Ref. 8.

Theory

A gas spring with an orifice is illustrated in Fig. 1. The piston is assumed to undergo a small-amplitude periodic motion that induces small perturbations in the enclosed gas. Mean gas properties

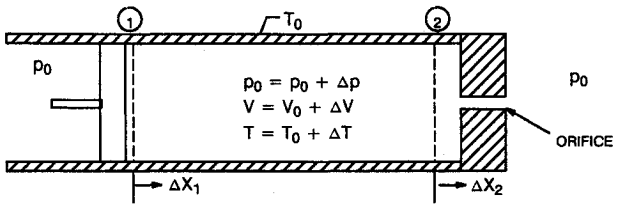

Fig. 1 Schematic representation of gas spring with orifice.

are denoted by a subscript 0. The walls of the gas spring are assumed to remain at temperature T_0.

Energy relations, heat transfer, orifice flow, and power dissipation are discussed in the following sections. First-order heat transfer equations are discussed in Appendix A. The second-order heat transfer associated with thin thermal boundary layers is discussed in Appendix B.

Energy Equation

Conservation of energy can be expressed in the form

$$\Delta Q = p\Delta V + \Delta E \tag{1}$$

In view of the nonuniform temperature distribution within the gas spring, the internal energy is expressed in terms of pressure, namely,

$$E = \int_0^V c_v \rho T \, dV = pV/(\gamma - 1) \tag{2}$$

where the perfect gas law $p = \rho RT$, and the relations $R = c_p - c_v$ and $\gamma = c_p/c_v$ have been used. Substitution of the differential of Eq. (2) into Eq. (1) yields

$$\frac{\Delta Q}{E_0} = \frac{\Delta p}{p_0} + \gamma \frac{\Delta V}{V_0} \tag{3}$$

where $E_0 = c_v \rho_0 T_0 V_0$. Equation (3) is the form of the energy equation used herein.

Heat Transfer

We consider the heat transfer associated with a fluid confined by parallel plates (Fig. 2). The case of cylindrical geometry is discussed in Appendix A. A sinusoidal pressure variation is assumed, and each dependent variable is expressed as the real part of a complex function. Thus, for pressure,

$$\frac{\Delta p}{p_0} = \frac{p_1}{p_0} \cos \omega t \tag{4a}$$

$$= \frac{p_1}{p_0} e^{i\omega t} \tag{4b}$$

where $p_1/p_0 \ll 1$ is assumed. Let $2r$ denote the separation between the two plates. The energy equation for a heat conducting gas, correct to terms of order $\Delta p/p_0$, is given by Eq. (A1). Convection terms are of order $(\Delta p/p_0)^2$ and are neglected in Eq. (A1). Integration of Eq. (A1) provides a first-order estimate for the variation of the temperature perturbation $\Delta T/T_0$ with s. The result, subject to the boundary condtions $\Delta T = 0$ at $s = r$ and $\partial \Delta T/\partial s = 0$ at $s = 0$, is

$$\frac{\gamma}{\gamma - 1} \frac{\Delta T/T_0}{\Delta p/p_0} = 1 - \frac{\cos(izs/r)}{\cos(iz)} \tag{5}$$

where $z = (1 + i)y$, $y = r/\lambda$, $\lambda = (2\bar{\alpha}/\omega)^{1/2}$, and $\bar{\alpha} = k/(\rho_0 c_p)$. The quantity λ is the thermal boundary-layer thickness associated with infinite plate separation. The net rate of heat transfer from gas to wall, $-\Delta \dot{Q}$, is found from $-\Delta \dot{Q}/S = -k(\partial \Delta T/\partial s)_w$. The result can be expressed

$$\frac{1}{G} \frac{p_0}{\Delta p} \left(\frac{-\Delta \dot{Q}}{\omega E_0} \right) = \frac{z \tanh z}{y^2} \tag{6a}$$

$$\equiv a + bi \tag{6b}$$

$$\equiv (a^2 + b^2)^{1/2} e^{i\Phi_q} \tag{6c}$$

where

$$G = \frac{\gamma - 1}{2} \frac{Sr}{V_0} \tag{7}$$

The choice $Sr/V_0 = 1$ is consistent with the parallel-plate geometry assumed by Eq. (5). The value $Sr/V_0 = 2$ applies to the cylindrical geometry discussed in Appendix A. It can be shown that Eqs. (5) and (6) apply for cases wherein $Sr/V_0 = 2$, provided $y \gg 1$.

The evaluation of Eq. (6a) is facilitated by noting

$$a + bi = \frac{(\sinh 2y - \sin 2y) + i(\sinh 2y + \sin 2y)}{y(\cosh 2y + \cos 2y)} \tag{8}$$

The limits $y \to 0$ and $y \to \infty$ correspond to isothermal and isentropic compressions, respectively. The expansion of Eq. (8) in these limits yields for $y \ll 1$

$$a = \frac{4}{3} y^2 \left[1 - \frac{68}{105} y^4 + 0(y^8) \right] \tag{9a}$$

$$b = 2 \left[1 - \frac{8}{15} y^4 + 0(y^8) \right] \tag{9b}$$

and for $y \gg 1$

$$a = b = \frac{1}{y} [1 + 0(e^{-2y})] \tag{10}$$

It follows that for $y \ll 1$

$$\Phi_q = \frac{\pi}{2} - \frac{2y^2}{3} + 0(y^4) \tag{11a}$$

$$\frac{|\Delta \dot{Q}/(\omega E_0)|}{p_1/p_0} = 2G \left[1 - \frac{14}{45} y^4 + 0(y^8) \right] \tag{11b}$$

and for $y \gg 1$

$$\Phi_q = \frac{\pi}{4} + 0(e^{-2y}) \tag{12a}$$

$$\frac{|\Delta \dot{Q}/(\omega E_0)|}{p_1/p_0} = \sqrt{2} \frac{G}{y} [1 + 0(e^{-2y})] \tag{12b}$$

The phase angle Φ_q decreases from the value $\pi/2$ at $y = 0$ to $\pi/4$ as $y \to \infty$. Since Φ_q is positive, the heat transfer rate from gas to wall leads the pressure perturbation. The ratio of the magnitude of the first-order heat transfer rate to the magnitude of the pressure perturbation varies from $2G$ at $y = 0$ to $\sqrt{2}G/y$ as $y \to \infty$. In the latter limit, the heat transfer is negligible. The parameter a approaches zero in the limits $y \to 0$ and $y \to \infty$ and has a maximum value at

$$y = 1.1271; \quad a = 0.8345; \quad b = 1.1633 \tag{13}$$

As previously noted, Eq. (5) represents a first-order solution to the equations that describe heat transfer from gas to wall due to a sinu-

soidal pressure variation. To this order, the heat transfer is also sinusoidal, and there is no net heat flux to the wall. However, the second-order solution to the heat transfer equations does indicate a finite transfer of heat, from gas to wall, per cycle. An alternate procedure for evaluating the second-order heat transfer to the wall is to evaluate the piston work per cycle. The latter procedure is used herein [see Eq. (22)].

Orifice Flow

The pressure external to the orifice is assumed to be p_0 (Fig. 1). The pressure differential across the orifice is Δp. The corresponding volume flow at station 2 can be expressed in the form

$$\frac{\gamma}{\omega}\frac{\Delta \dot{X}_2}{L_2} = K\frac{\Delta p}{p_0} \tag{14a}$$

For Poiseuille flow,

$$K = \gamma\pi p_0 R^4 N/(8\mu L\omega V_0) \tag{14b}$$

where R and N are the orifice radius and the number of orifices in the endwall. Numerical evaluation of Eq. (14b) is discussed in a later section. The use of a valve permits K to be varied.

Piston Motion

The relation between piston motion and pressure perturbation is deduced herein. The volumetric change associated with particle displacement at stations 1 and 2 is

$$\frac{\Delta V}{V_0} = \frac{\Delta V_1 + \Delta V_2}{V_0} = \frac{\Delta X_2}{L_2} - \frac{\Delta X_1}{L_1} \tag{15}$$

The particle (piston) displacement at station 1 is expressed in the form

$$\frac{\Delta X_1}{L_1} = \frac{X_1}{L_1}e^{i\omega t} \tag{16}$$

where X_1 is complex, in general. Differentiation of Eq. (15) yields

$$\frac{\Delta V}{V_0} = \frac{\Delta \dot{X}_2}{L_2} - \frac{\Delta \dot{X}_1}{L_1} \tag{17}$$

Similarly, differentiation of Eq. (3) yields

$$\gamma\frac{\Delta \dot{V}}{V_0} = -\frac{\Delta \dot{p}}{p_0} + \frac{\Delta \dot{Q}}{E_0} \tag{18}$$

Substitution of Eqs. (6), (14), (16), and (17) into Eq. (18) gives

$$\gamma\frac{\Delta X_1}{L_1} = [\alpha + i(-\beta)]\frac{\Delta p}{p_0} \tag{19a}$$

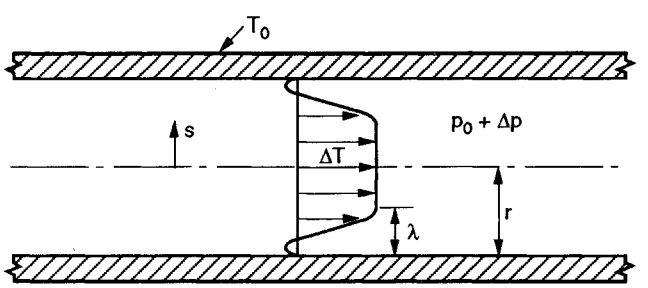

Fig. 2 Notation for thermal boundary-layer model. Case $y \equiv r/\lambda > 1$ is illustrated.

where

$$\alpha = 1 + Gb \tag{19b}$$

$$\beta = K + Ga \tag{19c}$$

An alternate form is

$$\gamma\frac{\Delta X_1}{L_1} = \sqrt{\alpha^2 + \beta^2}\,e^{i\Phi}\frac{\Delta p}{p_0} \tag{20a}$$

where

$$\Phi = \tan^{-1}(-\beta/\alpha) \tag{20b}$$

The phase angle Φ is in the fourth quadrant. Thus, the piston displacement lags the pressure perturbation. The ratio of piston displacement amplitude to pressure perturbation amplitude is

$$\frac{\gamma|X_1/L_1|}{p_1/p_0} = (\alpha^2 + \beta^2)^{1/2} \tag{20c}$$

Equations (19) and (20) permit perturbations to be expressed in terms of piston displacement ΔX_1, rather than pressure perturbation Δp, and are of primary interest in the present study.

The plot of pressure perturbation Δp vs piston displacement ΔX_1 is an ellipse whose coordinates move in a clockwise manner as t increases. The area of the ellipse is equal to the work done, per cycle, by the piston. This work is evaluated in the next section. At each value of ΔX_1, the pressure perturbation Δp is greater during the compression stroke than during the expansion stroke. It is this difference that leads to a finite piston work per cycle as well as the characterization of this work as a hysteresis effect.

Piston Power

The average power expended by the piston is denoted P and is found from

$$\frac{P}{A_1} = \frac{\omega}{2\pi}\int_0^{2\pi/\omega} \Delta p\Delta \dot{X}_1\,dt = 1/2\ R.P.[\Delta p\,(\Delta \dot{X}_1)^*] \tag{21}$$

where $R.P.$ denotes the real part. If the average power is normalized with respect to pressure perturbation amplitude, the evaluation of Eq. (21) yields

$$\frac{2\gamma}{\omega p_0 V_0}\frac{P}{(p_1/p_0)^2} = K + Ga \tag{22}$$

where K is the contribution of viscous dissipation within the orifice, and Ga is the contribution of the second-order heat transfer. These contributions are independent when P is normalized with respect to $(p_1/p_0)^2$, as in Eq. (22). The second-order heat transfer is zero in the limits $y \to 0, \infty$ and is a maximum at the value of y given in Eq. (13). Thus, as previously noted, the second-order heat transfer associated with a sinusoidal pressure variation has been evaluated by a consideration of piston power. For a thin thermal boundary layer, the second-order heat transfer can be related to the work done at the edge of the boundary layer by the isentropic core flow (e.g., Ref. 9). This is discussed in Appendix B.

In a gas spring, the piston displacement ΔX_1 is generally specified, and the corresponding pressure perturbation Δp is initially unknown. It is, therefore, desirable to normalize the piston power by piston displacement. Recall that ΔX_1 and Δp are related by Eqs. (20). A suitable normalization, denoted $\bar{P}$, is then

$$\bar{P} = \frac{4}{\gamma\omega p_0 V_0}\frac{P}{|X_1/L_1|^2} = \frac{2\beta}{\alpha^2 + \beta^2} \tag{23}$$

which can be expanded to yield

$$\bar{P} = \frac{2K}{\alpha^2 + \beta^2} + \frac{2Ga}{\alpha^2 + \beta^2} \tag{24}$$

Because of the factor $1/(\alpha^2 + \beta^2)$ in Eq. (24), the contributions of the orifice and the second-order heat transfer to $\bar{P}$ are no longer independent.

In the limits of small and large y, respectively,

$$\bar{P} = \frac{2\,[K + (4/3)\,Gy^2 + 0\,(y^6)\,]}{(1+2G)^2 + K^2 + (8/3)\,GKy^2 + 0\,(y^4)} \tag{25}$$

$$= \frac{2\,[K + (G/y) + 0\,(e^{-2y}/y)\,]}{1 + K^2 + (2G/y)\,(1+K) + 0\,(1/y^2)} \tag{26}$$

Optimum Power

If one considers the variation of $\bar{P}$ with K, at fixed y, a power maximum is found at $\beta = \alpha$, or

$$K_m = 1 + G(b - a) \tag{27a}$$

with a value

$$\bar{P}_m = 1/(1 + Gb) \tag{27b}$$

These quantities equal for $y \ll 1$

$$K_m = 1 + 2G[1 - (2/3)y^2 + 0(y^4)] \tag{28a}$$

$$\bar{P}_m = 1/\{1 + 2G[1 - (8/15)y^4 + o(y^8)]\} \tag{28b}$$

and for $y \gg 1$

$$K_m = 1 + 0(e^{-2y}/y) \tag{29a}$$

$$\bar{P}_m = 1/[1 + (G/y) + 0(e^{-2y}/y)] \tag{29b}$$

At the maximum power point, the phase of ΔX_1 relative to Δp has the fixed value

$$\Phi = -\pi/4 \tag{30}$$

Numerical Results

Numerical results for gas spring performance are presented in Figs. 3 and 4 for $G = 1/5$ and in Fig. 5 for $G = 1/3$. The values $G = 1/5$ and $1/3$ correspond to $\gamma = 7/5$ and $5/3$ when $Sr/V_0 = 1$. These results are now discussed with emphasis on power dissipation.

The variation of $\bar{P}$ with K, for fixed values of y, is given in Figs. 3a and 5a for $G = 1/5$ and $1/3$, respectively. For a given value of y, $\bar{P}$ is a maximum at a value of K near 1 in accord with Eqs. (27–29). When operating at an optimum value of K, a decrease in first-order heat transfer leads to an increase in $\bar{P}_m$. The maximum possible value of $\bar{P}$ is $\bar{P}_m = 1$, which occurs at $y \to \infty$, $K = 1$. In this limit, $\dot{Q} = 0$, and there is no contribution from heat transfer.

The variation of $\bar{P}$ with y, for fixed values of K, is indicated in Figs. 4a and 5b. The case $K = 0$ assumes no orifice flow and corresponds to the result reported in Ref. 1. When $K = 0$, $\bar{P} = 0$ in the limits $y \to 0$ and $y \to \infty$. A maximum in $\bar{P}$ occurs at a value of y of order 1. In particular, $\bar{P}_m = 0.224$ at y_m 1.301, and $\bar{P}_m = 0.301$ at $y_m = 1.399$ for $G = 1/5$ and $1/3$, respectively. In these cases ($K = 0$), the second-order heat transfer from the gas to the wall is the sole contributor to $\bar{P}_m$ and provides values of $\bar{P}_m$ that are about 22 and 30%, respectively, of the value one obtained for the isentropic case ($K = 1$, $y \to \infty$). The variation of $\bar{P}$ with y does not exhibit a local maximum for values of K in the range $K \geq 0$ (0.5). The maximum value of $\bar{P}$ in the limits $y \ll 1$ and $y \gg 1$ are found from $K = 1 + 2G$, $\bar{P} = 1/(1 + 2G)$, and $K = 1$, $\bar{P} = 1$, respectively.

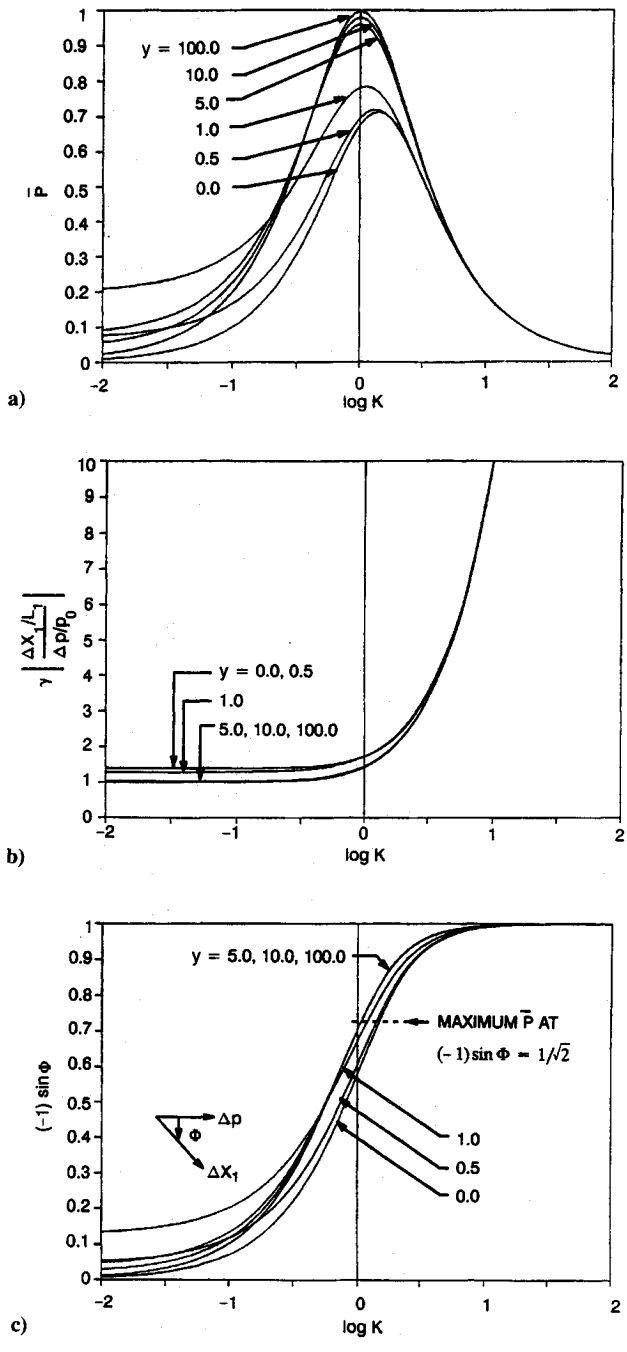

Fig. 3 Variation of gas spring performance with orifice area parameter K for fixed values of the normalized gas spring semiwidth parameter y, $G = 1/5$: a) normalized power $\bar{P}$ vs log K; b) ratio $\gamma|\Delta X_1/L_1|/|\Delta p/p_0|$ vs log K; and c) (-1) sin Φ vs log K.

A plot of $\gamma|\Delta X_1/L_1|/|\Delta p/p_0|$ vs K, for fixed values of y, is given in Fig. 3b. This parameter has the value one in the isentropic limit $y \to \infty$, $K = 0$ and increases, with increase in K, for obvious physical reasons. There is a relatively small increase in this parameter, with decreases in y, at fixed K.

Recall that Φ is the phase of ΔX_1 relative to Δp and is in the fourth quadrant. The variation of $-\sin \Phi$ with K, for fixed values of y, is indicated in Fig. 3c. The parameter $-\sin \Phi$ equals zero in the isentropic limit $y \to \infty$; $K = 0$ and increases to the value one with increase in K. The maximum power occurs at $\Phi = -\pi/4$. The dependence of $-\sin \Phi$ on y is relatively weak.

The amplitude and phase of the first-order heat transfer, relative to the pressure perturbation, is given in Figs. 4b and 4c. These quantities are independent of K. The first-order heat transfer decreases with increase in y (Fig. 4b), as expected. The phase angle

Φ_q has the value $\Phi_q = \pi/2$ at $y \ll 1$ and $\Phi_q = \pi/4$ at $y \gg 1$ in accord with Eqs. (11) and (12).

Evaluation of Parameters

Evaluation of K and y requires knowledge of gas viscosity μ and thermal diffusivity $\bar{\alpha}$. For air ($\gamma = 7/5$)

$$\mu = 1.716 \times 10^{-4}\left(\frac{T}{273}\right)^{0.78} \frac{\text{g}}{\text{cm}-\text{s}} \tag{31a}$$

$$\bar{\alpha} = \frac{1.859}{p_0\,(\text{atm})}\left(\frac{T}{273}\right)^{1.78} \frac{\text{cm}^2}{\text{s}} \tag{31b}$$

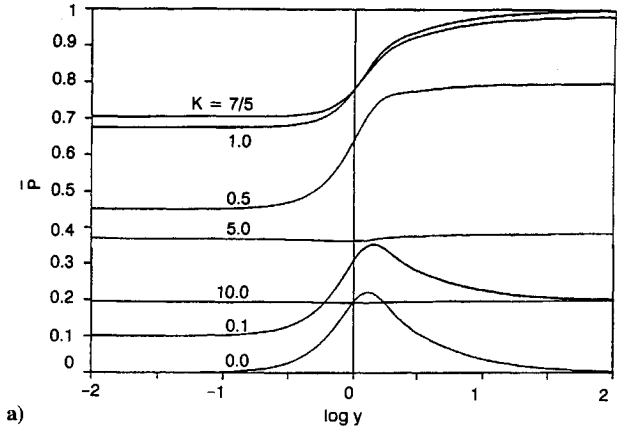

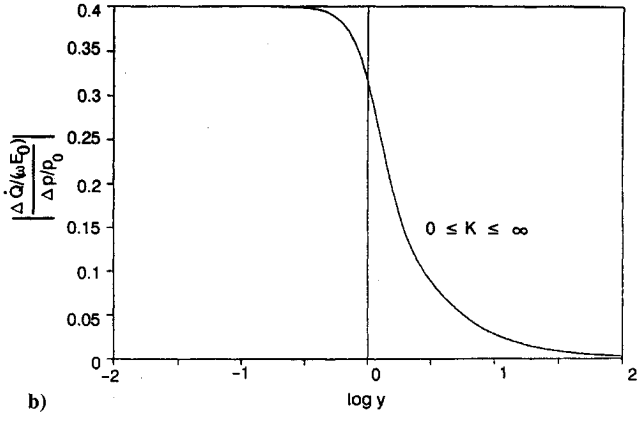

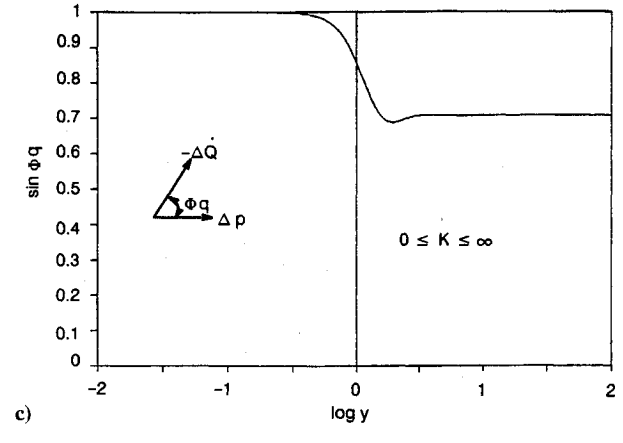

Fig. 4 Variation of gas spring performance with y for fixed values of K, G = 1/5: a) normalized power $\bar{P}$ vs log y; b) ratio $\gamma|\Delta\dot{Q}/(\omega E_0)|/|\Delta p/p_0|$ vs log y; and c) sin Φ_q vs log y.

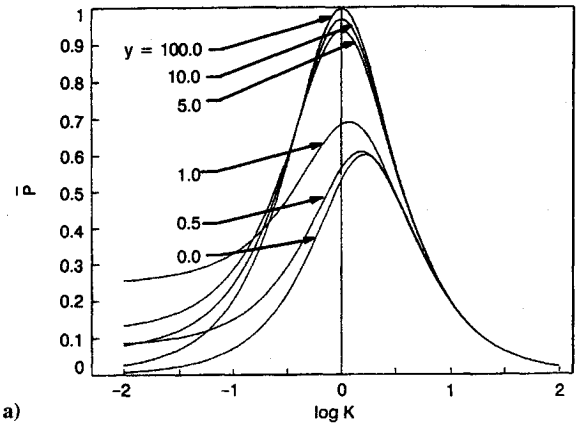

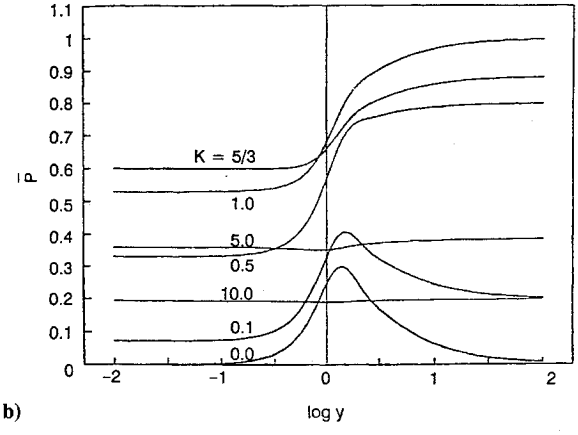

Fig. 5 Gas spring normalized power variation for G = 1/3: a) $\bar{P}$ vs log K and b) $\bar{P}$ vs log y.

and for helium ($\gamma = 5/3$)

$$\mu = 1.887 \times 10^{-4}\left(\frac{T}{273}\right)^{0.64} \frac{\text{g}}{\text{cm}-\text{s}} \tag{32a}$$

$$\bar{\alpha} = \frac{1.555}{p_0\,(\text{atm})}\left(\frac{T}{273}\right)^{1.64} \frac{\text{cm}^2}{\text{s}} \tag{32b}$$

The corresponding expressions for K (assuming Poiseuille flow) and y are

$$\left(\frac{L}{0.1}\right)\left(\frac{0.01}{R}\right)^4\left(\frac{\nu V_0}{N}\right)\frac{K}{p_0\,(\text{atm})} = 51.65\left(\frac{273}{T}\right)^{0.78} \text{Air} \tag{33a}$$

$$= 55.92\left(\frac{273}{T}\right)^{0.64} \text{Helium} \tag{33b}$$

and

$$\frac{1}{r\sqrt{\nu}}\frac{y}{\sqrt{p_0\,(\text{atm})}} = 1.300\left(\frac{273}{T}\right)^{0.89} \text{Air} \tag{34a}$$

$$= 1.421\left(\frac{273}{T}\right)^{0.82} \text{Helium} \tag{34b}$$

where geometric terms are in centimeters. The values R = 0.01 cm and L = 0.1 cm were used to normalize R and L in Eqs. (33). Small orifice sizes are needed to obtain values of K that are of order 1.

Typical operational parameters for the gas spring portion of a pulse tube cryocooler are[7] ν = 10 Hz, p_0 = 10 atm, T_0 = 300 K, r = 1.0 cm, and $L_1 = L_2$ = 10 cm. The corresponding value of y, for air

and helium, is of order 10, which indicates a relatively thin thermal layer.

Concluding Remarks

The combined effect of heat transfer and orifice flow on gas spring hysteresis has been investigated with emphasis on conditions leading to maximum dissipation. Small perturbations have been assumed.

The relation between piston displacement ΔX_1 and pressure perturbation Δp has been derived [Eqs. (19) and (20)]. When normalized with respect to the pressure perturbation, the piston power P depends on the separate contributions of orifice dissipation and second-order heat transfer [Eq. (22)]. A parameter $\bar{P}$ was introduced that represents piston power normalized with respect to piston displacement [Eq. (23)]. The contribution of orifice dissipation and second-order heat transfer to $\bar{P}$ are not independent [Eq. (24)] due to their mutural effect on the relation between Δp and ΔX_1.

The variation of the average piston power $\bar{P}$ with the orifice flow parameter K has a local maximum. When operating at a value of K, corresponding to maximum power, the effect of heat transfer is to decrease piston power.

In the absence of an orifice ($K = 0$), piston power is due entirely to the second-order heat transfer from gas to wall. In this case, for $G = 1/5$ and $1/3$, the piston power equals 22 and 30%, respectively, of the piston power obtained from an optimum value of K and isentropic flow.

Appendix A: First-Order Heat Transfer

Equations that define the first-order heat transfer for plane and cylindrical geometries are deduced herein.

If terms of order $\Delta p/p_0$ are retained, the energy equation for a gas subject to small sinusoidal pressure oscillations can be expressed

$$\left[\frac{1}{\xi^\sigma}\frac{\mathrm{d}}{\mathrm{d}\xi}\left(\xi^\sigma\frac{\mathrm{d}}{\mathrm{d}\xi}\right)+1\right]\left(\frac{\gamma}{\gamma-1}\frac{\Delta T/T_0}{\Delta p/p_0}\right) = 1 \tag{A1a}$$

where $\sigma = 0, 1$ for plane and cylindrical geometries, and

$$\xi = (-2i)^{1/2}\, ys/r = izs/r \tag{A1b}$$

Convection effects are of order $(\Delta p/p_0)^2$ and are omitted in Eq. (A1a). The boundary conditions are

$$\Delta T/T_0 = 0 \quad \text{at} \quad s = r \tag{A2a}$$

$$\frac{\partial \Delta T/T_0}{\partial s} = 0 \quad \text{at} \quad s = 0 \tag{A2b}$$

The temperature profile and the heat transfer for $\sigma = 0$ are given by Eqs. (5) and (6), respectively. The corresponding expressions for $\sigma = 1$ are

$$\frac{\gamma}{\gamma-1}\frac{\Delta T/T_0}{\Delta p/p_0} = 1-\frac{J_0(izs/r)}{J_0(iz)} \tag{A3a}$$

$$\frac{1}{G}\frac{p_0}{\Delta p}\left(\frac{-\Delta\dot{Q}}{\omega E_0}\right) = (-1)\frac{iz}{y^2}\frac{J_1(iz)}{J_0(iz)} \tag{A3b}$$

$$\equiv a + ib \tag{A3c}$$

where $J_n(\xi)$ denotes the Bessel function of order n. Limiting values of $a + ib$ are for $y \ll 1$

$$a + ib = \left(\frac{y^2}{4}+i\right)[1+0(y^4)] \tag{A4a}$$

and for $y \gg 1$

$$a + ib = \frac{1+i}{y}[1+0(e^{-2y})] \tag{A4b}$$

Equation (A4b) agrees with Eq. (10), as expected. The limit $y \gg 1$ corresponds to a thin boundary layer, and, in this limit, Eq. (6) is applicable for arbitrary geometries, provided an appropriate value of Sr/V_0 is used.

Appendix B: Second-Order Heat Transfer

For a thin thermal boundary layer ($y \gg 1$), the second-order heat transfer can be related to the work done on the boundary layer by the isentropic core flow (e.g., Ref. 9). This is illustrated in the present appendix.

Integration of the continuity equation indicates that the vertical velocity v at the edge of the boundary layer is

$$v = \frac{\partial}{\partial t}\int_s^r\left(\frac{\Delta p}{p_0}-\frac{\Delta T}{T_0}\right)\mathrm{d}s \tag{B1a}$$

$$= \frac{1}{\gamma}(r-s)\frac{\Delta\dot{p}}{p_0}+\frac{V_0}{\gamma s}\left(\frac{-\Delta\dot{Q}}{E_0}\right) \tag{B1b}$$

The integration of $\Delta T/T_0$ is accomplished with the aid of Eqs. (A1). The first term in Eq. (B1b) represents an isentropic compression. The second term in Eq. (B1b) describes the contribution of the heat transfer rate $\Delta\dot{Q}$ to v. The average rate of work done by the core flow on the boundary layer is

$$P = 1/2\ R.P.[Sv(\Delta p)^*] \tag{B2a}$$

$$= Ga[\omega p_0 V_0 (p_1/p_0)^2/(2\gamma)] \tag{B2b}$$

which agrees with Eq. (22). The second-order heat transfer is seen to be proportional to the real part of the product $(-\Delta\dot{Q})(\Delta p)^*$. This result is true, in general, as is seen in Eqs. (6) and (22). The isentropic compression term in Eq. (B1b) does not contribute.

References 9 and 10 discuss the heat transfer associated with acoustic waves in tubes. A solution of the second-order heat transfer equations is presented in Ref. 10. The present study, with $K = 0$, corresponds to the endwall region in Refs. 9 and 10.

Acknowledgment

The present study was supported by The Aerospace Corporation's Sponsored Research program.

References

[1]Lee, K. P., "A Simplistic Model of Cyclic Heat Transfer Phenomena in Closed Spaces," *Proceedings of the 18th Intersociety Energy Conversion Engineering Conference*, IEEE, Boston, 1983, pp. 720–723.

[2]Kornhauser, A. A., and Smith, J. L., Jr., "The Effects of Heat Transfer on Gas Spring Performance," *Proceedings of the 26th Intersociety Energy Conversion Engineering Conference*, Vol. 5, IEEE, Boston, 1991, pp. 180–185.

[3]Ureili, I., and Berkowitz, D. M., *Stirling Cycle Engine Analysis*, Adam Hilger Ltd., Bristol, England, UK, 1984, pp. 127–135.

[4]Kornhauser, A. A., "Dynamic Modeling of Gas Springs," *Proceedings of the 26th Intersociety Energy Conversion Engineering Conference*, Vol. 5, IEEE, Boston, 1991, pp. 176–179.

[5]Walker, G., *Cryocooler, Part I: Fundamentals*, Plenum Press, New York, 1983, pp. 170, 171.

[6]Mikulin, E. L., Tarasov, A. A., and Shkrebyonock, M. P., "Low Temperature Expansion Pulse Tubes," *Advances in Cryogenic Engineering*, Vol. 29, Plenum Press, New York, 1984, p. 629.

[7]Storch, P. J., Radebaugh, R., and Zimmerman, J. E., "Analytical Model for the Refrigeration Power of the Orifice Pulse Tube Refrigerator," National Inst. of Standards and Technology, TN 1343, 1990.

[8]Mirels, H., "Linearized Theory for Pulse Tube Cryocooler Performance," *AIAA Journal*, Vol. 32, No. 8, pp. 1662–1669.

[9]Rott, N., "Thermoacoustics," *Advances in Applied Mechanics*, Vol. 20, Academic Press, New York, 1980, pp. 135–175.

[10]Merkli, P., and Thomann, H., "Thermoacoustic Effects in a Resonance Tube," *Journal of Fluid Mechanics*, Vol. 70, Pt. I, 1975, pp. 161–177.